The influence of true polar wander on glacial inception in North America

A. Daradich [a,*], P. Huybers [b], J.X. Mitrovica [b], N.-H. Chan [c,1], J. Austermann [b]

[a] *Department of Earth and Environmental Sciences, University of Ottawa, Ottawa, Ontario, Canada*
[b] *Department of Earth and Planetary Sciences, Harvard University, Cambridge, MA, USA*
[c] *Lunar and Planetary Laboratory, University of Arizona, Tucson, AZ, USA*

A B S T R A C T

The impact that long-term changes in Earth's rotation axis relative to the surface geography, or true polar wander (TPW), and continental drift have had in driving cooling of high-latitude North America since the Eocene is explored. Recent reanalyses of paleomagnetic pole positions suggest a secular drift in Earth's rotation axis of ~8° over the last 40 Myr, in a direction that has brought North America to increasingly higher latitudes. Using modern temperature data in tandem with a simple model, a reduction in the annual sum of positive degree days (PDDs) driven by this polar and plate motion over the last 20 Myr is quantified. At sites in Baffin Island, the TPW- and continental drift-driven decrease in insolation forcing over the last 20 Myr rivals changes in insolation forcing caused by variations in Earth's obliquity and precession. Using conservative PDD scaling factors and an annual snowfall equal to modern station observations, the snowiest location in Baffin Island 20 Myr ago had a mass balance deficit of ~0.75–2 m yr^{-1} (water equivalent thickness) relative to its projected mass balance at 2.7 Ma. This mass balance deficit would have continued to increase as one goes back in time until ~40 Myr ago based on adopted paleopole locations. TPW and continental drift that moved Arctic North America poleward would have strongly promoted glacial inception in Baffin Island at ~3 Ma, a location where the proto-Laurentide Ice Sheet is thought to have originated.

© 2017 The Authors. Published by Elsevier B.V. This is an open access article under the CC BY-NC-ND license (http://creativecommons.org/licenses/by-nc-nd/4.0/).

1. Introduction

The fossil record in North America shows evidence of a long-term secular cooling over the past 65 Myr. This cooling began at a time when much of Earth's climate was relatively warm and culminated in the glacial cycles of the Pleistocene. In contrast to the polar desert with sparse vegetation that exists today, 50 Myr ago flora and fauna in the northernmost islands of the Canadian Arctic Archipelago reflected the presence of a temperate climate with high rainfall (e.g., Francis, 1988; McKenna, 1980; Basinger et al., 1994). Compilations of oxygen isotope (δ^{18}O) values from benthic foraminerfera found in globally-distributed deep-sea cores also provide evidence of a global secular cooling trend throughout the Cenozoic (e.g., Zachos et al., 2001). Oxygen isotope values record changes in both deep-sea temperatures and ice volume (e.g., Shackleton, 1987), and show

variability over a range of timescales. In addition to an observed long-term trend, oxygen isotope values show higher frequency variability (10^4–10^6 yr) that is related to changes in Earth's orbital parameters, i.e., precession, obliquity, eccentricity (e.g., Hays et al., 1976; Imbrie et al., 1992). While changes in the amount and distribution of insolation driven by variations in Earth's orbital parameters have been correlated with glacial and interglacial cycles (Milankovitch, 1941; Imbrie et al., 1992; Huybers and Wunsch, 2005), these changes in insolation alone appear not to have been responsible for glacial inception in North America ~3 Ma (Shackleton and Opdyke, 1977). In particular, orbital solutions indicate generally consistent insolation variability over the last 30 Myr (Laskar et al., 2004), and minimum values for Northern Hemisphere insolation during the Pleistocene are comparable to those seen at earlier times during the Cenozoic.

Other mechanisms thought to have played a role in shaping Cenozoic climate include changes in the concentration of atmospheric greenhouse gases, and a number of slow processes that are tectonic in origin. Long-term records show a large (>500 ppm) and variable decline in atmospheric CO_2 concentrations since 50 Ma, reaching values below 500 ppm after ~25 Ma that have been

relatively stable in comparison to the aforementioned decline (Pearson and Palmer, 2000; Pagani et al., 2005; Beerling and Royer, 2011; Zhang et al., 2013; Martínez-Botí et al., 2015). Numerical modeling suggests that declining levels of atmospheric CO_2 could have been an important driving mechanism for Cenozoic glaciation of Antarctica ∼34 Ma (DeConto and Pollard, 2003), and an intensification of Northern Hemisphere glaciation during the Plio-Pleistocene Transition (Lunt et al., 2008; Willeit et al., 2015). A sharp decline in atmospheric CO_2 on the order of 100 ppm could have led to conditions favorable for glacial inception in North America through reduced radiative forcing during the Plio-Pleistocene Transition (PPT). However, whether such a decline occurred is difficult to establish with confidence given that different estimates of CO_2 spanning the same time period are uncertain to within at least 200 ppm (e.g., Pagani et al., 2010; Seki et al., 2010; Willeit et al., 2015). As for the role of CO_2 in driving long-term Cenozoic climate change, a clearer link exists during the early Cenozoic when declining levels of atmospheric CO_2 were coincident with a long-term secular cooling trend. However, during the late Oligocene and Miocene, atmospheric pCO_2 was relatively low and stable during periods of both high-latitude cooling and global warming (Pagani et al., 2005; Zhang et al., 2013).

Tectonic processes are plausible candidates as drivers for climate change over long timescales, since these are inherently linked to mantle convection, a process that evolves over millions of years. Movement of the Earth's tectonic plates drives continental drift and sea-floor spreading, which reflect horizontal motions, as well as vertical displacements caused by rifting and orogeny. Mantle flow can also drive large-scale vertical displacements of the Earth's tectonic plates, known as dynamic topography (Hager, 1984; Mitrovica et al., 1989; Gurnis, 1992). Changes in paleogeography could have had an important effect on the observed global cooling of Cenozoic climate by altering oceanic and atmospheric circulation (e.g., Raymo, 1994). Tectonically driven events thought to be responsible for such changes include the opening of a circum-Antarctic seaway (Kennett, 1977; Lawver and Gahagan, 2003) and elevation of both the Tibetan–Himalayan and Sierra–Coloradan regions (Ruddiman and Raymo, 1988). In addition, uplift of the Tibetan plateau could have led to higher erosion rates, resulting in increased carbon sequestration and subsequent cooling of global climate (Raymo and Ruddiman, 1992). Prior to the closure of the Indonesian seaway 3–4 Myr ago, a warmer eastern tropical Pacific and permanent El Niño state could have increased heat transport to North America through atmospheric teleconnections (Cane and Molnar, 2001; Huybers and Molnar, 2007). The creation of the Isthmus of Panama during the Pliocene, and its impact on ocean circulation, have also been cited as a mechanism for Northern Hemisphere cooling and glaciation (Driscoll and Haug, 1998; Haug and Tiedemann, 1998), however the significance and precise timing of these events remain highly contentious (Molnar, 2008).

The mechanisms described above may have acted together to drive Cenozoic cooling, and numerical modeling has provided some insight into their relative importance. For example, Bradshaw et al. (2012) used a fully coupled atmosphere–ocean–vegetation simulation to examine the effect of changing paleogeography and atmospheric CO_2 concentrations in reproducing late Miocene climate. They found that while changing paleogeography did impact their results, atmospheric CO_2 concentrations at the higher end of the range of estimates were required to explain a warmer late Miocene climate relative to present-day.

In this paper we consider another process that has the potential to significantly alter climate, namely true polar wander (TPW), and focus on its possible role in the inception of North American glaciation. TPW refers to a motion of the rotation axis relative to the Earth's surface and it has a direct impact on climate by changing the latitude (and thus insolation history) of all points on the surface. This process has previously been proposed as a mechanism for secular cooling of North America during the Cenozoic (Donn and Shaw, 1977), however paleomagnetic inferences of TPW from the 1970s (Jurdy and Van der Voo, 1975) suggested that polar motion, and its effect on climate, would have been minor since the beginning of the Cenozoic. In this paper we revisit this possible connection using a recently updated estimate of TPW since the Late Cretaceous and simple models of North American climate.

2. True polar wander and climate

In addition to changes in a planet's rotation axis in space (e.g., obliquity, precession), large excursions of the rotation axis relative to the surface geography are possible (Gold, 1955; Goldreich and Toomre, 1969). This reorientation of the rotation pole, or TPW, results from any mass redistribution within the Earth system, and it occurs over a wide range of time scales. For example, ice age surface mass (ice plus ocean) flux, and the associated glacial isostatic adjustment of the solid Earth, drives TPW with time scales of 10^3–10^5 yr (e.g., Sabadini and Peltier, 1981; Wu and Peltier, 1984). This ice-age-induced polar motion is characterized by relatively small (∼0.1°) oscillatory changes in Earth's rotation axis, with no secular component (Chan et al., 2015). In contrast, the redistribution of density heterogeneities within the Earth's mantle by thermo-chemical convection can drive large amplitude (>10°) oscillatory (Creveling et al., 2012) and secular (e.g., Spada et al., 1992; Ricard et al., 1993; Steinberger and O'Connell, 1997; Doubrovine et al., 2012) TPW with time scales of order 10^6–10^9 yr. These excursions of the rotation axis have been inferred from paleomagnetic measurements and they have occurred throughout geological time (e.g., Van der Voo, 1994; Evans, 1998; Maloof et al., 2006; Mitchell et al., 2010). Moreover, they have been linked to major changes in global climate and geochemical cycles (Hoffman, 1999; Li et al., 2004; Maloof et al., 2006).

Changes in the position of North America relative to the Earth's rotation axis through the Cenozoic result from both TPW and continental drift. The net direction of this motion brings North America increasingly poleward (e.g., Jurdy and Van der Voo, 1975; Besse and Courtillot, 2002; O'Neill et al., 2005; Torsvik et al., 2012; Doubrovine et al., 2012). Early studies using climate models of varying sophistication (e.g., Donn and Shaw, 1977; Barron, 1985) concluded that the observed cooling of North American climate during the Cenozoic could not be explained by net changes in paleogeography alone. This result led Donn and Shaw (1977) to speculate that a larger contribution from TPW was required in order to explain the observed cooling trend. At the time of these studies, paleomagnetically inferred pole positions suggested TPW of less than a few degrees since 65 Ma (Jurdy and Van der Voo, 1975).

In order to simultaneously estimate plate motions and TPW from paleomagnetic data, these data must be evaluated relative to a specific frame of reference. The analysis by Jurdy and Van der Voo (1975) adopted the hotspot reference frame which assumes that hotspots are relatively stationary with respect to the Earth's mantle (Morgan, 1972). Using a recent compilation of paleomagnetic data that significantly increases the number of constraints on TPW (Torsvik et al., 2012), and an iterative analysis procedure that permits the drift of hotspots, Doubrovine et al. (2012) have inferred a secular drift in Earth's rotation axis of ∼8° since 40 Ma in the so-called global moving hotspot reference frame (GMHRF; Fig. 1). Their estimated TPW path indicates a progressive displacement of the Earth's rotation axis toward Greenland over the last 40 Myr.

To better illustrate North America's changing location during the Cenozoic, paleogeography at 30 Ma in the GMHRF (including
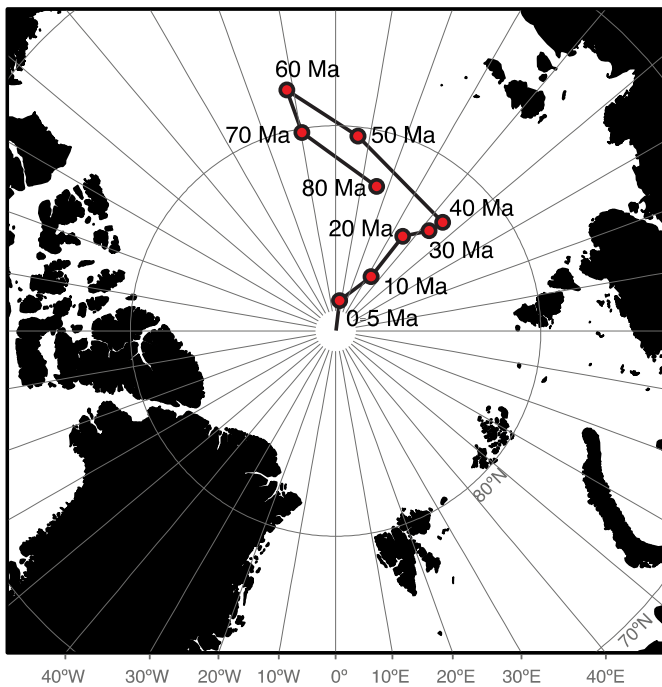
Fig. 1. Mean paleopole positions from Doubrovine et al. (2012).

plate motion and TPW) relative to present-day is shown in Fig. 2. The paleogeography shown depicts backward rotated and translated modern-day coastlines, and therefore includes features due to glacial erosion that would not have existed prior to the Quaternary. Notably, the Great Lakes, Hudson's Bay and the channels that separate the islands of the Canadian Arctic Archipelago (Dowsett et al., 2016). This paleogeography reconstruction is consistent with the general consensus that North America has been moving poleward over the last 40 Myr (e.g., Jurdy and Van der Voo, 1975; Besse and Courtillot, 2002; O'Neill et al., 2005; Torsvik et al., 2012;

Doubrovine et al., 2012). Although the exact position of each paleopole in Fig. 1 has large uncertainty, the growing evidence that recent TPW has been of larger amplitude than previously thought indicates that the possible connection between plate motions, TPW and North American climate should be revisited. Indeed, a recent study has suggested that solid-Earth processes, including TPW, over the last 60 Ma may have contributed to the build-up of the Greenland ice sheet (Steinberger et al., 2015). Our focus is the Canadian Arctic, the site of glacial inception of the massive Laurentide Ice Sheet (by far the largest of the North American ice sheets) at 3 Ma. In the following, we use modern climatological data in tandem with simple climate models to estimate TPW-driven changes in positive degree days (PDDs) for this region over the last 20 Myr. This metric allows us to directly compare the impact of TPW to other mechanisms that perturb the number of PDDs, such as changes in Earth's orbital parameters.

3. Modern climatological gradients

The formation of glaciers occurs when snow persists in the same location throughout the year. To achieve this positive mass balance, annual accumulation of precipitation must exceed ablation caused by positive temperatures. In order to investigate the effect TPW might have had on glacial inception in North America, we begin by examining modern climatological gradients in both temperature and precipitation. Daily temperature data are taken from a second generation homogenized dataset for sites in Canada (Vincent et al., 2012) and the Global Historical Climate Network (GHCN) (Peterson and Vose, 1997) for sites in the US and Greenland. Mean daily temperature values for both datasets are calculated by averaging maximum and minimum daily temperatures. Mean daily temperature data for the years 1950–2012 is then standardized to an elevation of 0 m using a constant lapse rate of $5.6\,^\circ\mathrm{C\,km^{-1}}$. This value was adopted by Kleman et al. (2013) in their study of Northern Hemisphere ice sheet formation, and it is consistent with calculated lapse rates for glaciers in the Canadian high Arctic, which are typically lower than average observed
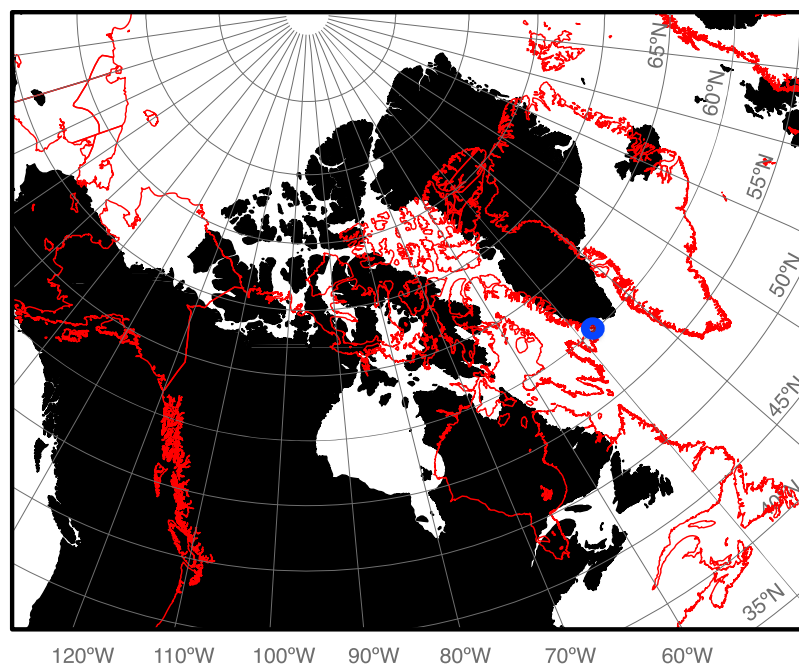

Fig. 2. Paleogeography of North America at 30 Ma (red) relative to present-day. Plate reconstructions were computed in a GMHRF using GPlates. The contribution to paleogeography from TPW is computed using the 30 Ma paleopole shown in Fig. 1. The location of Cape Dyer, Baffin Island, is indicated by a blue circle. (For interpretation of the references to color in this figure legend, the reader is referred to the web version of this article.)
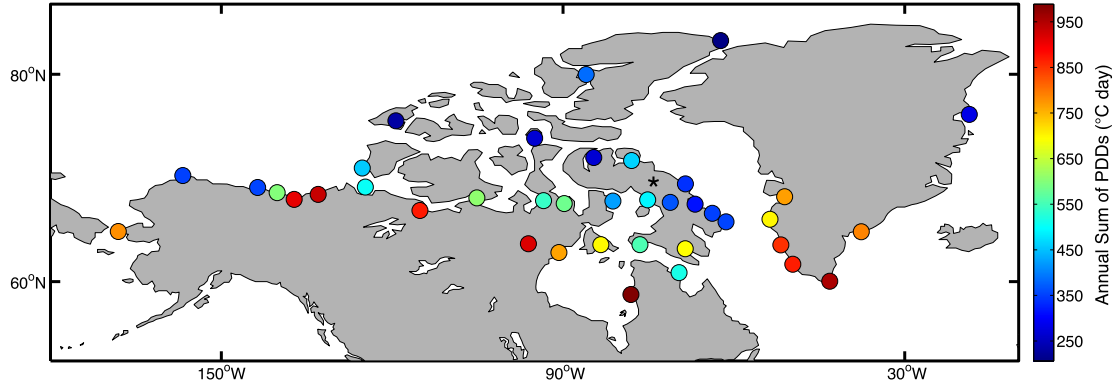
Fig. 3. Average annual sum of positive degree days (PDDs) at present-day for sites with values less than 1000 °C-day (minimum value, 206 °C-day). Temperatures are standardized to 0 m elevation (see text). The location of Baffin Island is highlighted by an asterisk. (For interpretation of the colors in this figure, the reader is referred to the web version of this article.)
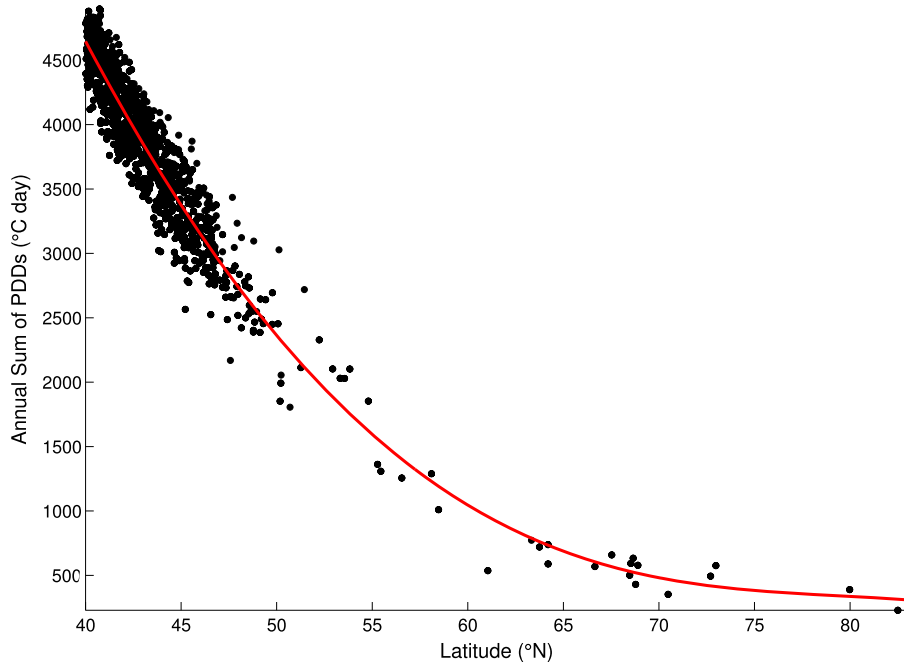
Fig. 4. Average annual sum of PDDs for sites between 60–90°W at present-day. (For interpretation of the references to color in this figure, the reader is referred to the web version of this article.)

lapse rates in the lower troposphere of 6–7 °C km^{-1} (Gardner et al., 2009). The standardized mean daily temperatures are then used to calculate the average annual sum of PDDs for sites with at least 30 yr of data, as shown in Fig. 3. This annual sum is defined as:

$$\text{PDD} = \sum \delta_d T_d, \qquad \delta_d = \begin{cases} 1, & \text{if } T_d > 0\,^\circ\text{C} \\ 0, & \text{otherwise} \end{cases} \qquad (1)$$

where T_d is the mean daily temperature.

The annual sum of PDDs is commonly used as a measure of the influence of near-surface temperature on annual ablation (Braithwaite and Zhang, 2000). As expected, there is a large increase in PDDs at progressively lower latitudes. To highlight this dependence, Fig. 4 shows the same average annual sum of PDDs as in Fig. 3 as a function of latitude, for sites between 60–90°W. The red curve in the figure represents the least-squares polynomial of degree 3 that best fits the data. This range of longitudes coincides with the present-day location of Baffin Island in the Canadian Arctic Archipelago, its location highlighted by an asterisk in Fig. 3. As we discuss below, there is evidence that the proto-Laurentide ice

sheet originated within Baffin Island, and this motivates our focus on this location.

While PDDs increase as a function of decreasing latitude, changes in mass balance resulting from TPW could be affected by a coincident change in precipitation. Average annual snowfall (mm water equivalent (w.e.) thickness) for the years 1950–2012 is shown in Fig. 5a. Only sites that have at least 20 yr of data are shown (all sites in the Canadian Arctic have at least 30 yr of data). Data for Canadian sites is taken from the second generation Adjusted Precipitation for Canada (APC2) dataset (Mekis and Vincent, 2011) and for sites in the US and Greenland we adopt the GHCN database. Fig. 5b shows average annual snowfall data for all GHCN and APC2 sites located between 60–90°W and above 40°N (i.e., the same range of longitudes and latitudes shown in Fig. 4). The site with by far the greatest annual snowfall in Baffin Island is Cape Dyer, indicated by a red circle in Fig. 5b. Unlike changes in PDDs, changes in precipitation do not show a simple latitudinal dependence. As a first estimate of the effect of polar wander on mass balance (i.e., accumulation vs. ablation), we compare the range in values for average annual snowfall shown in Fig. 5b to

(a)

(b)
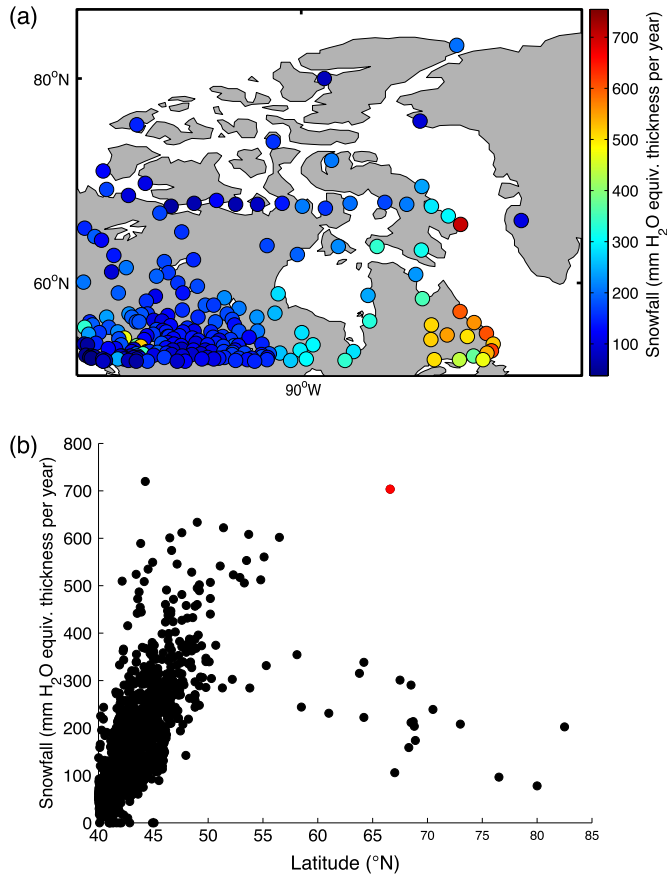
Fig. 5. (a) Average annual snowfall (mm H$_2$O equivalent thickness) at present-day. Only sites that have at least 20 yr of data are shown (all sites in the Canadian Arctic have at least 30 yr of data). (b) Same as in (a) for sites between 60–90°W. Snowfall at Cape Dyer, Baffin Island, is indicated by a red circle. (For interpretation of the references to color in this figure legend, the reader is referred to the web version of this article.)

changes in PDDs as a function of latitude given by the red curve in Fig. 4. For this exercise, we assume a present-day location of 65°N in Baffin Island (Baffin Island is located between 63–73°N) and a paleolatitude for this location of 60°N. A 5° change in latitude for our chosen site is less than the change in latitude over the last 30 Myr dictated by the paleogeography shown in Fig. 2. The change in PDDs by moving from 65°N to 60°N along the curve in Fig. 4 is 360 °C-day. Scaling factors that relate PDDs to ablation rates (in mm w.e. thickness), based on experimental observations, range from 3–8 mm °C^{-1} day^{-1} for snow and ice (Braithwaite and Zhang, 2000). Using these scaling factors, we predict an increase in ablation of 1080–2880 mm w.e. by moving from 65–60°N, which far exceeds any coincident increase in snowfall that might have occurred based on the range of values shown in Fig. 5b. This suggests that TPW will have a significantly greater impact on ablation than on snowfall (i.e., accumulation).

4. Insolation and summer energy

Forcing of Pleistocene glaciation through changes in orbital configuration is often characterized by quantifying radiation received over some portion of the year at a given latitude. Various conventions include averaging over that half of the year in which the most radiation is received (Milankovitch, 1941), averaging insolation on a single day such as June 21st (Imbrie et al., 1992), or summing insolation above a fixed radiation threshold (Huybers, 2006). Here we adopt the approach used by Huybers and Molnar (2007) of transforming insolation to temperature through the use

of a simple, linear model and then calculating PDDs. In particular, the seasonal cycle of temperature is fit at each station i using a lag, L, sensitivity, S, and constant temperature, B:

$$T_i(d + L) = S_i I(d, \phi_i) + B_i \qquad (2)$$

where T_i is the lagged daily mean temperature and $I(d, \phi_i)$ is the daily average insolation as a function of both day and latitude.

Huybers and Molnar (2007) demonstrated that results from this model were comparable to those obtained by fitting an energy-balance-model. They also argued that the relationship between temperature and insolation in Eq. (2), which was based on modern conditions, should hold to first order under different orbital configurations, since "variations in insolation are small relative to the mean and are concentrated at the seasonal cycle". We note that this model does not include climate feedbacks, however the importance of such mechanisms is reduced because we focus on conditions leading up to glacial inception. Thus, consideration of changes in surface albedo associated with ice sheet growth is obviated, although other feedbacks could amplify (or damp) responses, including those associated with seasonal snow cover, water vapor, and clouds (e.g., Jochum et al., 2012).

Using the average of mean temperature for each day of the year (with no correction for elevation) at GHCN and Canadian sites north of 40°N with at least 30 yr of data, we fit Eq. (2) to find values for L, S and B at each station (Fig. 6). The average cross-correlation between Eq. (2) and the average seasonal cycle smoothed to monthly resolution at each site is 0.99, while the average residual variance is 3.0. We then calculate the daily average insolation at each site (Berger, 1978) for obliquity values of 24.2° and 22.2°. Again, assuming that Eq. (2) holds under different orbital conditions, these insolation values (along with values for L, S and B) are used to calculate daily mean temperatures, which are then input to Eq. (1) to calculate annual PDDs. The calculated difference in annual PDDs between high- and low-obliquity states (24.2° and 22.2°) is shown in Fig. 7. The difference in annual PDDs increases with increasing latitude, where obliquity-induced changes in insolation are the highest. We also see greater variability in ΔPDD in the high-Canadian arctic, with values for sites in Baffin Island varying between ∼(150–250) ΔPDD. Given that such changes in obliquity were evidently sufficient to transition between glacial and interglacial states during the Early Pleistocene (e.g., Imbrie et al., 1992), when glacial cycles occurred at the obliquity period, this range provides a measure of the threshold in ΔPDD that needs to be surpassed in order for glaciation of the Canadian Arctic to occur, and we return to it when we explore the possible impact of TPW on glacial inception in North America.

5. Glacial inception and mass balance

The Pleistocene ice age was marked by a long series of glacial cycles. At times of maximum glaciation, the Laurentide Ice Sheet reached as far south as 40°N (Dyke et al., 2002). Inception of the Laurentide Ice Sheet within each cycle is thought to have occurred in one of three locations: Keewatin, Labrador–Ungava and Baffin Island (Dyke, 2009). There is strong evidence to suggest that Baffin Island must have played a particularly important role in the initiation of ice cover. For example, at present-day, the eastern coast of Baffin Island is characterized by high elevation and alpine mountains that are glaciated, and the topography trends lower toward the southwest. This topography leaves Baffin Island prone to glaciation, since a modest lowering of the present-day snowline by 300 m would encompass a large area of the island that is presently unglaciated (Williams, 1978). Additionally, the absence of lichen in large areas of Baffin Island shows that a movement westward of perennial snow cover occurred during the "Little Ice Age" (∼300 yr ago) (Andrews et al., 1976). This is
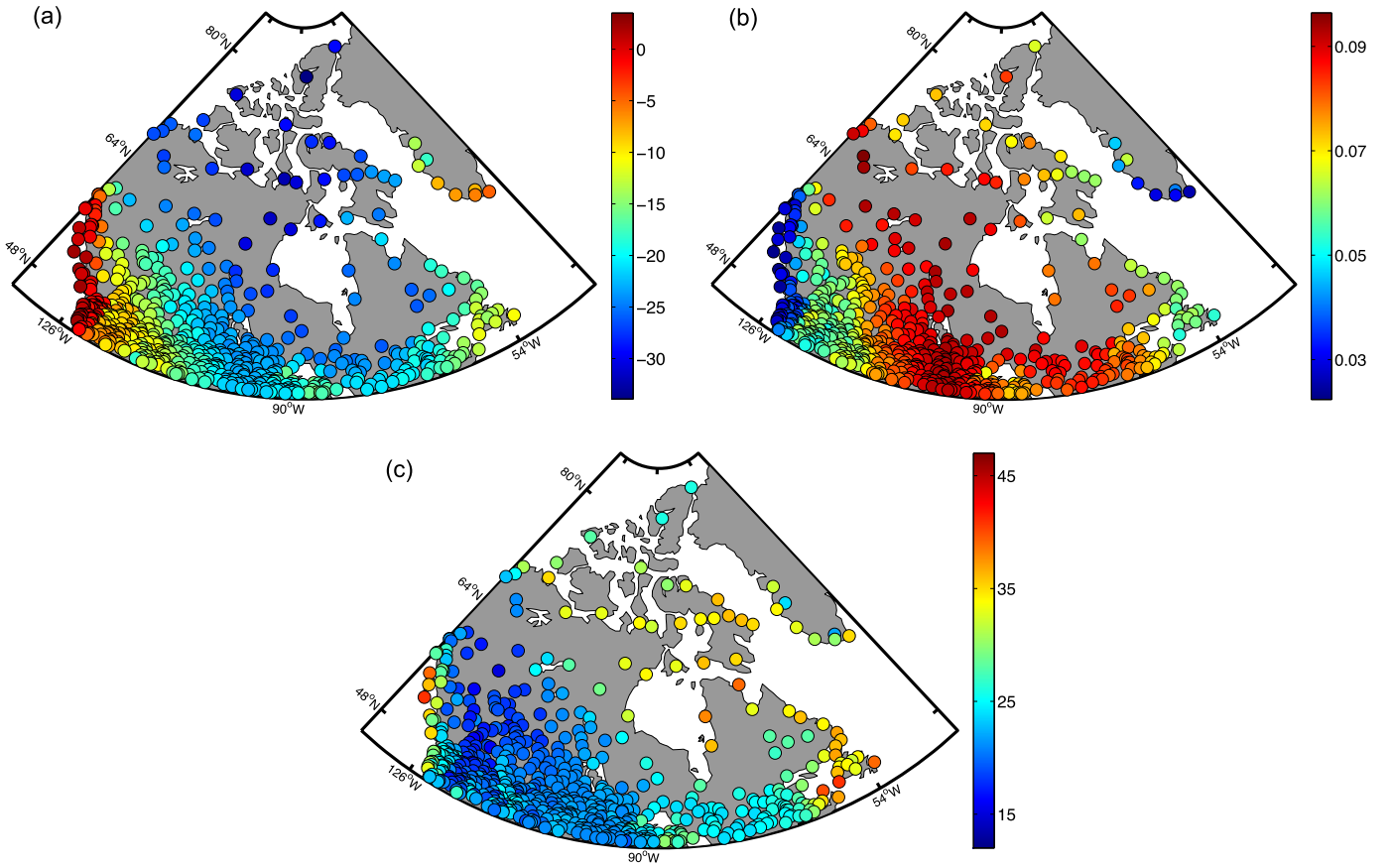
Fig. 6. Parameters in Eq. (2) that characterize the response of temperature to changes in insolation at sites North of 40°N. (a) *B*, in units of °C. (b) Sensitivity of temperature to insolation, *S*, in units of °C m² W⁻¹. (c) Number of days temperature lags insolation, *L*. (For interpretation of the colors in this figure, the reader is referred to the web version of this article.)
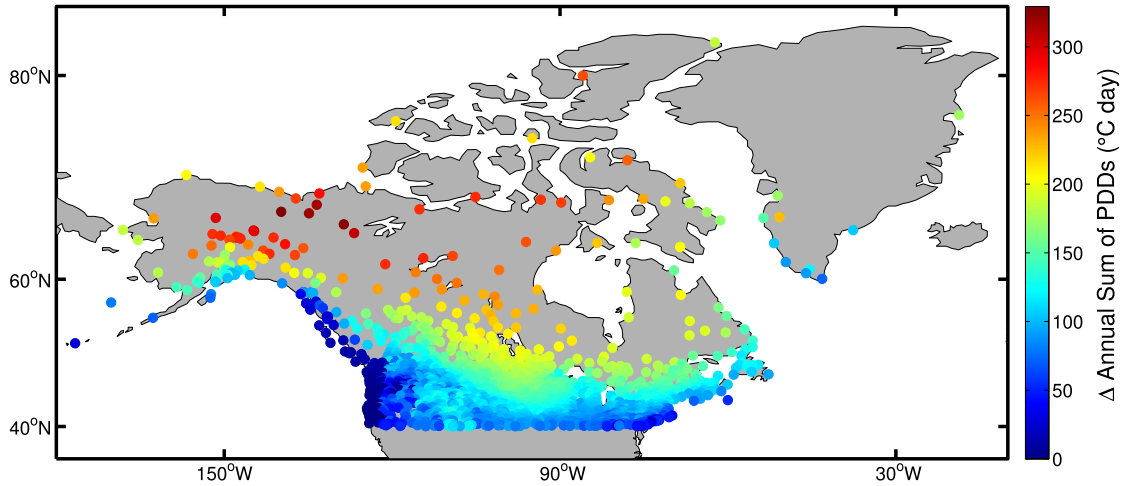

Fig. 7. Difference in annual sum of PDDs for high- and low-obliquity orbital conditions, 22.2° and 24.2°. (For interpretation of the colors in this figure, the reader is referred to the web version of this article.)

noteworthy, since the little ice age snowline on Baffin Island is only 100–200 m higher than large plateaus of the Canadian Arctic to the west of Baffin Island. In addition, numerical simulations of varying complexity pinpoint Baffin Island as the initial site of glacial inception for the Laurentide ice sheet during the last interglacial to glacial transition, ∼115,000 yr ago (e.g., Williams, 1979; Otieno and Bromwich, 2009; Vavrus et al., 2011; Jochum et al., 2012). We note that present-day Baffin Island was not separated from the main landmass by a waterway prior to the Quaternary, and was not an island at this time. Therefore, references to "Baffin Island" prior to the Quaternary refer to the area of land that now forms this island.

To model changes in PDDs at sites in Baffin Island over the last 20 Myr, we begin with values that were obtained by fitting Eq. (2) to modern temperature data, as described in the previous section. Using Canadian sites with at least 30 yr of data, values estimated for sites in Baffin Island range from −29.0 to −22.8 °C for *B*, 31–36 days for *L* and 0.061–0.078 °C m² W⁻¹ for *S*. Using Eq. (2) and insolation values from an orbital solution valid for the last 50 Myr (Laskar et al., 2004), we calculate daily mean temper-
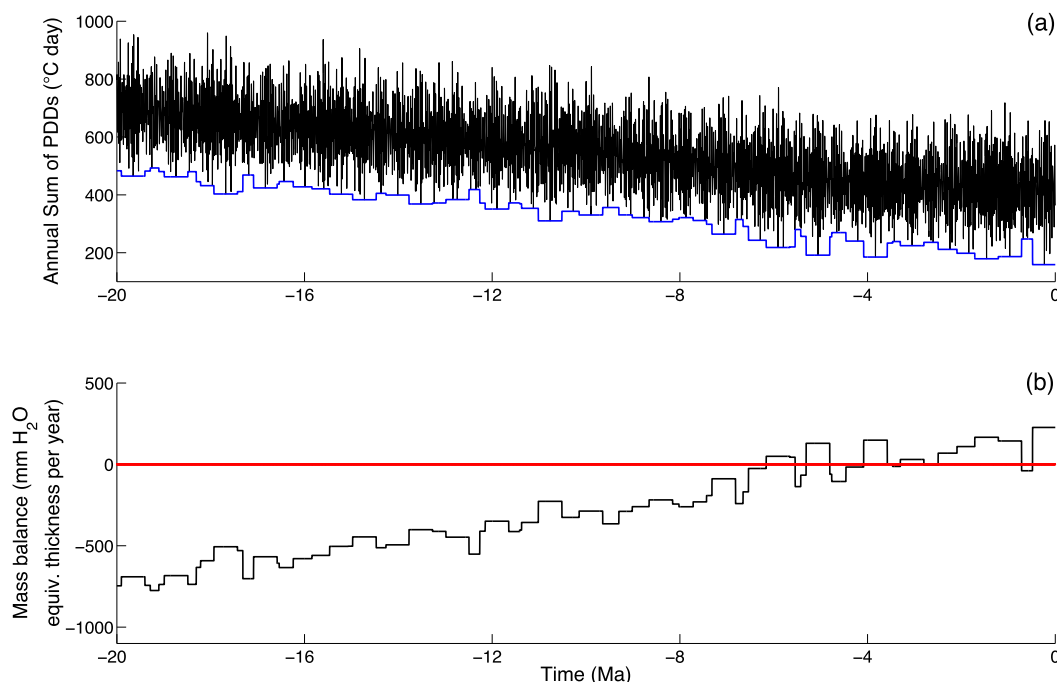
Fig. 8. (a) Annual sum of PDDs at Cape Dyer, Baffin Island since 20 Ma, with a running 501-kyr minimum shown in blue. These minimum values are used to calculate (b) the corresponding mass balance for a PDD-ablation scaling factor of 3 mm/day °C. Zero mass balance (i.e., annual ablation is equal to total annual snowfall) is indicated by a red line. The values reflect changes in PDDs due to past orbital configurations, TPW and continental drift. (For interpretation of the references to color in this figure legend, the reader is referred to the web version of this article.)

atures for the year at 1-kyr intervals over the last 20 Myr, and in turn use these temperatures to calculate an annual sum of PDDs. We then superimpose a change in PDDs as a function of latitude dictated by the red curve in Fig. 4. The latitude of a given site as a function of time (including plate motion and TPW) is calculated using GPlates (www.gplates.org). Plate ID assignments and associated rotation poles used in the software are given by Müller et al. (2008), and these have been modified to include TPW in the GMHRF assuming the paleopole positions shown in Fig. 1.

The choice to use values in Eq. (2) calculated for modern-day station locations, and then superimpose a change in PDDs as a function of latitude was motivated by the complex spatial structure of values for both S and L, which do not show a simple latitudinal dependence. This result is expected, since the influence of solar radiation on the annual cycle of surface air temperatures depends on a number of factors which include a site's proximity to land or ocean and atmospheric circulation patterns (e.g., North et al., 1983; McKinnon et al., 2013). We note that we also calculated changes in PDDs at sites in Baffin Island over the last 20 Myr using Eq. (2) and insolation values that varied as a function of both time and paleolatitude of a given location. For this exercise, we assume modern-day values for both S and L, however we impose a change in B as a function of latitude. Although there is also a complex spatial structure associated with values for B, we generally expect cooler temperatures at higher latitudes, and therefore fit a linear trend ($m = -0.51$ °C/°lat, $r^2 = 0.54$) to values of this variable for sites located between 60–90°W and above 40°N. Changes in PDDs over the last 20 Myr calculated using this method are consistent with the first method of superimposing a change in PDDs as a function of latitude (results not shown).

The results of our analysis for the easternmost station in Baffin Island, Cape Dyer ($B = -27$ °C, $L = 28$ days, $S = 0.054$ °C m^2 W^{-1}), which records the highest average annual snowfall in the region (~700 mm w.e.), are shown in Fig. 8. To best demonstrate the potential significance of TPW, we choose this station as it is where it would be most difficult to achieve a negative mass balance caused

by a change in paleolatitude. Values for PDDs in Fig. 8a are for the response at Cape Dyer to the full insolation variability plus the effects of TPW. A trend in the minimum value obtained across multiple orbital cycles is also indicated (blue curve), and highlights how TPW moves the system closer to a threshold for glacial inception. The magnitude of this TPW-induced trend in minimum PDDs over the last 20 Myr surpasses the ~160 °C-day change in PDDs between Earth's high- and low-obliquity conditions (Fig. 7) and nears the ~400 °C-day range induced by the combination of obliquity and precession variability when eccentricity is large (Fig. 8a). These orbital benchmarks indicate that TPW could play a first-order role in priming the system for glaciation.

Minimum values for PDDs shown in Fig. 8a were used to calculate the mass balance shown in Fig. 8b. In calculating the mass balance, we assume a conservative PDD scaling factor of 3 mm °C^{-1} day^{-1} and an annual snowfall equal to modern station observations. Zero mass balance (i.e., annual ablation is equal to total annual snowfall) is indicated by a red line in Fig. 8b. With these values, we find a negative mass balance in Cape Dyer at 20 Ma that is ~0.75 m/yr (w.e.). This value depends on the ablation scaling factor used, and a mass balance deficit of ~2 m/yr (w.e.) relative to 2.7 Ma is found for 8 mm °C^{-1}day^{-1}. While there is uncertainty associated with the PDD scaling factor used, calculated mass balance deficits at 20 Ma are large relative to the present-day annual precipitation received at this station of ~700 mm w.e. It is important to note that while only the last 20 Myr are shown, mass balance deficits would have increased until at least 40 Ma based on the paleopole positions in Fig. 1.

6. Conclusions

Our simple models find that even a modest rate of TPW (~0.2 deg/Myr) in tandem with plate tectonic motion would have resulted in cooling that contributed significantly to glacial inception in North America at ~3 Ma. The snowiest location in Baffin Island at 20 Ma had a mass balance deficit of ~0.75–2 m/yr (w.e.)

relative to its projected mass balance at 2.7 Ma. While we have focused our study on sites in Baffin Island, the entire North American continent would have been affected by TPW in a spatially dependent manner.

Climate change driven by TPW would work together with other mechanisms that prime the system for glaciation, such as reductions in atmospheric CO_2 (Lunt et al., 2008; Willeit et al., 2015) or changes in ocean circulation (Cane and Molnar, 2001; Huybers and Molnar, 2007). Despite their potentially having disparate time scales, CO_2, ocean, and tectonic processes may together bring the system near enough to a threshold for glaciation whereby favorable orbital conditions would activate positive snow and ice-albedo feedbacks (e.g., Jochum et al., 2012). Another possibility is that changes in atmospheric circulation played a role. In this regard, the southern drift of Alaska and the Russian Far East (Chukotka) away from the polar region, and the contemporaneous northward migration of the Canadian Arctic, may have had significant effects on atmospheric circulation and snowfall rates on Baffin Island. Exploring this issue will require more sophisticated climate modeling; this is beyond the scope of the present study, but will be the subject of future work. Such modeling should also explore the issue of why regions such as Alaska and the Russian Far East appear to have been ice free prior to their southward migration.

An independent study has recently suggested that solid-Earth processes, including TPW, over the last 60 Ma have led to conditions favorable for the build-up of the Greenland ice sheet (Steinberger et al., 2015). The effect of these processes on regional temperatures or glacial mass balance in Greenland have yet to be quantified, but our results suggest that the impact of TPW could have been significant. In any event, this article, together with the present study, highlight the important role that long-term processes linked to mantle dynamics might have played in shaping Earth's climate over millions of years.

Acknowledgements

References

Andrews, J.T., Davis, P.T., Wright, C., 1976. Little Ice Age Permanent snowcover in the Eastern Canadian Arctic: extent mapped from LANDSAT-1 satellite imagery. Geogr. Ann., Ser. A, Phys. Geogr. 58 (1/2), 71–81.

Barron, E.J., 1985. Explanations of the Tertiary global cooling trend. Palaeogeogr. Palaeoclimatol. Palaeoecol. 50, 45–61. http://dx.doi.org/10.1016/S0031-0182(85)80005-5.

Basinger, J.F., Greenwood, D.R., Sweda, T., 1994. Early Tertiary vegetation of Arctic Canada and its relevance to paleoclimatic interpretation. In: Boulter, M.C., Fisher, H.C. (Eds.), Cenozoic Plants and Climates of the Arctic. In: NATO ASI Ser., vol. 127. Springer-Verlag, pp. 175–198.

Beerling, D.J., Royer, D.L., 2011. Convergent Cenozoic CO_2 history. Nat. Geosci. 4, 418–420. http://dx.doi.org/10.1038/ngeo1186.

Berger, A.L., 1978. Long-term variations of daily insolation and quaternary climatic changes. J. Atmos. Sci. 35, 2362–2367.

Besse, J., Courtillot, V., 2002. Apparent and true polar wander and the geometry of the geomagnetic field over the last 200 Myr. J. Geophys. Res. 107 (B11), 2300. http://dx.doi.org/10.1029/2000JB000050.

Bradshaw, C.D., Lunt, D.J., Flecker, R., Salzmann, U., Pound, M.J., Haywood, A.M., Eronen, J.T., 2012. The relative roles of CO_2 and palaeogeography in determining late Miocene climate: results from a terrestrial model-data comparison. Clim. Past 8, 1257–1285. http://dx.doi.org/10.5194/cp-8-1257-2012.

Braithwaite, R.J., Zhang, Y., 2000. Sensitivity of mass balance of five Swiss glaciers to temperature changes assessed by tuning a degree-day model. J. Glaciol. 46 (152), 7–14. http://dx.doi.org/10.3189/172756500781833511.

Cane, M.A., Molnar, P., 2001. Closing of the Indonesian seaway as a precursor to east African acidification around 3–4 million years ago. Nature 411, 157–162.

Chan, N.-H., Mitrovica, J.X., Daradich, A., 2015. Did glacially induced TPW end the ice age? A reanalysis. Geophys. J. Int. 202, 1749–1759. http://dx.doi.org/10.1093/gji/ggv230.

Creveling, J.R., Mitrovica, J.X., Chan, N.-H., Latychev, K., Matsuyama, I., 2012. Mechanisms for oscillatory true polar wander. Nature 491, 244–248. http://dx.doi.org/10.1038/nature11571.

DeConto, R.M., Pollard, D., 2003. Rapid Cenozoic glaciation of Antarctica induced by declining atmospheric CO_2. Nature 421, 245–249.

Donn, W.L., Shaw, D.M., 1977. Model of climate evolution based on continental drift and polar wandering. Geol. Soc. Am. Bull. 88, 390–396.

Doubrovine, P.V., Steinberger, B., Torsvik, T.H., 2012. Absolute plate motions in a reference frame defined by moving hot spots in the Pacific, Atlantic, and Indian oceans. J. Geophys. Res. 117, 1–30. http://dx.doi.org/10.1029/2011JB009072.

Dowsett, H., Dolan, A., Rowley, D., Moucha, R., Forte, A.M., Mitrovica, J.X., Pound, M., Salzmann, U., Robinson, M., Chandler, M., Foley, K., Haywood, A., 2016. The PRISM4 (mid-Piacenzian) paleoenvironmental reconstruction. Clim. Past 12, 1519–1538.

Driscoll, N.W., Haug, G.H., 1998. A short circuit isn thermohaline circulation: a cause for Northern Hemisphere glaciation? Science 282, 436–438.

Dyke, A.S., 2009. Laurentide ice sheet. In: Gornitz, V. (Ed.), Encyclopedia of Paleoclimatology and Ancient Environments. Springer, Netherlands, pp. 517–520.

Dyke, A.S., Andrews, J.T., Clark, P.U., England, J.H., Miller, G.H., Shaw, J., Veillette, J.J., 2002. The Laurentide and Innuitian ice sheets during the Last Glacial Maximum. Quat. Sci. Rev. 21, 9–31. http://dx.doi.org/10.1016/S0277-3791(01)00095-6.

Evans, D.A., 1998. True polar wander, a supercontinental legacy. Earth Planet. Sci. Lett. 157, 1–8. http://dx.doi.org/10.1016/S0012-821X(98)00031-4.

Francis, J.E., 1988. A 50-million-year-old fossil forest from Strathcona Fiord, Ellesmere Island, Arctic Canada: evidence for a warm polar climate. Arctic 41 (4), 314–318.

Gardner, A.S., Sharp, M.J., Koerner, R.M., Labine, C., Boon, S., Marshall, S.J., Burgess, D.O., Lewis, D., 2009. Near-surface temperature lapse rates over Arctic glaciers and their implications for temperature downscaling. J. Climate 22, 4281–4298. http://dx.doi.org/10.1175/2009JCLI2845.1.

Gold, T., 1955. Instability of the Earth's axis of rotation. Nature 175, 526–529. http://dx.doi.org/10.1038/175642b0.

Goldreich, P., Toomre, A., 1969. Some remarks on polar wandering. J. Geophys. Res. 74 (10), 2555–2567.

Gurnis, M., 1992. Rapid continental subsidence following the initiation and evolution of subduction. Science 255, 1556–1558. http://dx.doi.org/10.1126/science.255.5051.1556.

Hager, B.H., 1984. Subducted slabs and the geoid: constraints on mantle rheology and flow. J. Geophys. Res. 89 (B7), 6003–6015. http://dx.doi.org/10.1029/JB089iB07p06003.

Haug, G.H., Tiedemann, R., 1998. Effect of the formation of the Isthmus of Panama on Atlantic Ocean thermohaline circulation. Nature 393, 673–676. http://dx.doi.org/10.1038/31447.

Hays, J.D., Imbrie, J., Shackleton, N.J., 1976. Variations in the Earth's orbit: pacemaker of the Ice Ages. Science 194, 1121–1132. http://dx.doi.org/10.1126/science.194.4270.1121.

Hoffman, P.F., 1999. The break-up of Rodinia, birth of Gondwana, true polar wander and the snowball Earth. J. Afr. Earth Sci. 28 (1), 17–33. http://dx.doi.org/10.1016/S0899-5362(99)00018-4.

Huybers, P., 2006. Early Pleistocene glacial cycles and the integrated summer insolation forcing. Science 313, 508–511. http://dx.doi.org/10.1126/science.1125249.

Huybers, P., Molnar, P., 2007. Tropical cooling and the onset of North American glaciation. Clim. Past 3, 549–557. http://dx.doi.org/10.5194/cpd-3-771-2007.

Huybers, P., Wunsch, C., 2005. Obliquity pacing of the late Pleistocene glacial terminations. Nature 434, 491–494. http://dx.doi.org/10.1038/nature03349.1.2.3.4.5.6.Luiten.

Imbrie, J., Boyle, E.A., Clemens, S.C., Duffy, A., Howard, W.R., Kukla, G., Kutzbach, J., Martinson, D.G., McIntyre, A., Mix, A.C., Molfino, B., Morley, J.J., Peterson, L.C., Pisias, N.G., Prell, W.L., Raymo, M.E., Shackleton, N.J., Toggweiler, J.R., 1992. On the structure and origin of major glacial cycles: 1. Linear responses to Milankovitch forcing. Paleoceanography 7 (6), 701–738. http://dx.doi.org/10.1029/93pa02751.

Jochum, M., Jahn, A., Peacock, S., Bailey, D.A., Fasullo, J.T., Kay, J., Levis, S., Otto-Bliesner, B., 2012. True to Milankovitch: glacial inception in the new community climate system model. J. Climate 25, 2226–2239. http://dx.doi.org/10.1175/JCLI-D-11-00044.1.

Jurdy, D.M., Van der Voo, R., 1975. True polar wander since the Early Cretaceous. Science 187, 1193–1196. http://dx.doi.org/10.1126/science.187.4182.1193.

Kennett, J.P., 1977. Cenozoic evolution of Antarctic glaciation, the circum-Antarctic Ocean, and their impact on global paleoceanography. J. Geophys. Res. 82 (27), 3843–3860. http://dx.doi.org/10.1029/JC082i027p03843.

Kleman, J., Fastook, J., Ebert, K., Nilsson, J., Caballero, R., 2013. Pre-LGM Northern Hemisphere ice sheet topography. Clim. Past 9, 2365–2378. http://dx.doi.org/10.5194/cp-9-2365-2013.

Laskar, J., Robutel, P., Joutel, F., Gastineau, M., Correia, A.C.M., Levrard, B., 2004. A long-term numerical solution for the insolation quantities of the Earth. Astron. Astrophys. 428, 261–285. http://dx.doi.org/10.1051/0004-6361:20041335.

Lawver, L.A., Gahagan, L.M., 2003. Evolution of Cenozoic Seaways in the circum-Antarctic region. Palaeogeogr. Palaeoclimatol. Palaeoecol. 198, 11–37. http://dx.doi.org/10.1016/S0031-0182(03)00392-4.

Li, Z.X., Evans, D.A.D., Zhang, S., 2004. A 90° spin on Rodinia: possible causal links between the Neoproterozoic supercontinent, superplume, true polar wander and low-latitude glaciation. Earth Planet. Sci. Lett. 220, 409–421. http://dx.doi.org/10.1016/S0012-821X(04)00064-0.

Lunt, D.J., Foster, G.L., Haywood, A.M., Stone, E.J., 2008. Late Pliocene Greenland glaciation controlled by a decline in atmospheric CO_2 levels. Nature 454, 1102–1105. http://dx.doi.org/10.1038/nature07223.

Maloof, A.C., Halverson, G.P., Kirschvink, J.L., Schrag, D.P., Weiss, B.P., Hoffman, P.F., 2006. Combined paleomagnetic, isotopic, and stratigraphic evidence for true polar wander from the Neoproterozoic Akademikerbreen Group, Svalbard, Norway. Geol. Soc. Am. Bull. 118 (9/10), 1099–1124. http://dx.doi.org/10.1130/B25892.1.

Martínez-Botí, M.A., Foster, G.L., Chalk, T.B., Rohling, E.J., Sexton, P.F., Lunt, D.J., Pancost, R.D., Badger, M.P.S., Schmidt, D.N., 2015. Plio-Pleistocene climate sensitivity evaluated using high-resolution CO_2 records. Nature 518, 49–54. http://dx.doi.org/10.1038/nature14145.

McKenna, M.C., 1980. Eocene paleolatitude, climate, and mammals of Ellesmere Island. Palaeogeogr. Palaeoclimatol. Palaeoecol. 30, 349–362. http://dx.doi.org/10.1016/0031-0182(80)90065-6.

McKinnon, K.A., Stine, A.R., Huybers, P., 2013. The spatial structure of the annual cycle in surface temperature: amplitude, phase, and Lagrangian history. J. Climate 26, 7852–7862. http://dx.doi.org/10.1175/JCLI-D-13-00021.1.

Mekis, E., Vincent, L.A., 2011. An overview of the second generation adjusted daily precipitation dataset for trend analysis in Canada. Atmos.-Ocean 49 (2), 163–177. http://dx.doi.org/10.1080/07055900.2011.583910.

Milankovitch, M., 1941. Kanon der Erdbestrahlung und seine Anwendung auf das Eiszeitenproblem. Königlich Serbische Akademie.

Mitchell, R.N., Evans, D.A.D., Kilian, T.M., 2010. Rapid Early Cambrian rotation of Gondwana. Geology 38 (8), 755–758. http://dx.doi.org/10.1130/G30910.1.

Mitrovica, J.X., Beaumont, C., Jarvis, G.T., 1989. Tilting of continental interiors by the dynamical effects of subduction. Tectonics 8 (5), 1079–1094. http://dx.doi.org/10.1029/TC008i005p01079.

Molnar, P., 2008. Closing of the Central American Seaway and the Ice Age: a critical review. Paleoceanography 23, 1–15. http://dx.doi.org/10.1029/2007PA001574.

Morgan, W.J., 1972. Deep mantle convection plumes and plate motions. Am. Assoc. Pet. Geol. Bull. 56 (2), 203–213.

Müller, R.D., Sdrolias, M., Gaina, C., Roest, W.R., 2008. Age, spreading rates, and spreading asymmetry of the world's ocean crust. Geochem. Geophys. Geosyst. 9 (4), 1–19. http://dx.doi.org/10.1029/2007GC001743.

North, G.R., Mengel, J.G., Short, D.A., 1983. Simple energy balance model resolving the seasons and the continents: application to the astronomical theory of the Ice Ages. J. Geophys. Res., Oceans 88 (C11), 6576–6586. http://dx.doi.org/10.1029/JC088iC11p06576.

O'Neill, C., Müller, D., Steinberger, B., 2005. On the uncertainties in hot spot reconstructions and the significance of moving hot spot reference frames. Geochem. Geophys. Geosyst. 6 (4), 1–35. http://dx.doi.org/10.1029/2004GC000784.

Otieno, F.O., Bromwich, D.H., 2009. Contribution of atmospheric circulation to inception of the Laurentide Ice Sheet at 116 kyr BP. J. Climate 22, 39–57. http://dx.doi.org/10.1175/2008JCLI2211.1.

Pagani, M., Zachos, J.C., Freeman, K.H., Tipple, B., Bohaty, S., 2005. Marked decline in atmospheric carbon dioxide concentrations during the Paleogene. Science 309, 600–603. http://dx.doi.org/10.1126/science.1110063.

Pagani, M., Liu, Z., LaRiviere, J., Ravelo, A.C., 2010. High Earth-system climate sensitivity determined from Pliocene carbon dioxide concentrations. Nat. Geosci. 3, 27–30. http://dx.doi.org/10.1038/ngeo724.

Pearson, P.N., Palmer, M.R., 2000. Atmospheric carbon dioxide concentrations over the past 60 million years. Nature 406, 695–699. http://dx.doi.org/10.1038/35021000.

Peterson, T.C., Vose, R.S., 1997. An overview of the global historical climatology network temperature database. Bull. Am. Meteorol. Soc. 78 (12), 2837–2849. http://dx.doi.org/10.1175/JTECH-D-11-00103.1.

Raymo, M.E., 1994. The initiation of Northern Hemisphere glaciation. Annu. Rev. Earth Planet. Sci. 22, 353–383. http://dx.doi.org/10.1146/annurev.earth.22.1.353.

Raymo, M.E., Ruddiman, W.F., 1992. Tectonic forcing of late Cenozoic climate. Nature 359, 117–122.

Ricard, Y., Spada, G., Sabadini, R., 1993. Polar wandering of a dynamic earth. Geophys. J. Int. 113, 284–298. http://dx.doi.org/10.1111/j.1365-246X.1993.tb00888.x.

Ruddiman, W.F., Raymo, M.E., 1988. Northern Hemisphere climate regimes during the past 3 Ma: possible tectonic connections. Philos. Trans. R. Soc. Lond. B 318, 411–430. http://dx.doi.org/10.1098/rstb.1988.0017.

Sabadini, R., Peltier, W.R., 1981. Pleistocene deglaciation and the Earth's rotation: implications for mantle viscosity. Geophys. J. R. Astron. Soc. 66, 553–578.

Seki, O., Foster, G.L., Schmidt, D.N., Mackensen, A., Kawamura, K., Pancost, R.D., 2010. Alkenone and boron-based Pliocene pCO_2 records. Earth Planet. Sci. Lett. 292, 201–211. http://dx.doi.org/10.1016/j.epsl.2010.01.037.

Shackleton, N.J., 1987. Oxygen isotopes, ice volume and sea level. Quat. Sci. Rev. 6, 183–190. http://dx.doi.org/10.1016/0277-3791(87)90003-5.

Shackleton, N.J., Opdyke, N.D., 1977. Oxygen isotope and palaeomagnetic evidence for early Northern Hemisphere glaciation. Nature 270, 216–219. http://dx.doi.org/10.1038/270216a0.

Spada, G., Ricard, Y., Sabadini, R., 1992. Excitation of true polar wander by subduction. Nature 360, 452–454. http://dx.doi.org/10.1038/360452a0.

Steinberger, B., O'Connell, R.J., 1997. Changes of the Earth's rotation axis owing to advection of mantle density heterogeneities. Nature 387, 169–173. http://dx.doi.org/10.1038/387169a0.

Steinberger, B., Spakman, W., Japsen, P., Torsvik, T.H., 2015. The key role of global solid-Earth processes in preconditioning Greenland's glaciation since the Pliocene. Terra Nova 27, 1–8. http://dx.doi.org/10.1111/ter.12133.

Torsvik, T.H., Van der Voo, R., Preeden, U., Mac Niocaill, C., Steinberger, B., Doubrovine, P.V., van Hinsbergen, D.J.J., Domeier, M., Gaina, C., Tohver, E., Meert, J.G., McCausland, P.J.A., Cocks, L.R.M., 2012. Phanerozoic polar wander, palaeogeography and dynamics. Earth-Sci. Rev. 114, 325–368. http://dx.doi.org/10.1016/j.earscirev.2012.06.007.

Van der Voo, R., 1994. True polar wander during the middle Paleozoic? Earth Planet. Sci. Lett. 122, 239–243. http://dx.doi.org/10.1016/0012-821X(94)90063-9.

Vavrus, S., Philippon-Berthier, G., Kutzbach, J.E., Ruddiman, W.F., 2011. The role of GCM resolution in simulating glacial inception. Holocene 21 (5), 819–830. http://dx.doi.org/10.1177/0959683610394882.

Vincent, L.A., Wang, X.L., Milewska, E.J., Wan, H., Yang, F., Swail, V., 2012. A second generation of homogenized Canadian monthly surface air temperature for climate trend analysis. J. Geophys. Res. 117, 1–13. http://dx.doi.org/10.1029/2012JD017859.

Willeit, M., Ganopolski, A., Calov, R., Robinson, A., Maslin, M., 2015. The role of CO_2 decline for the onset of Northern Hemisphere glaciation. Quat. Sci. Rev. 119, 22–34. http://dx.doi.org/10.1016/j.quascirev.2015.04.015.

Williams, L.D., 1978. The Little Ice Age glaciation level on Baffin Island, Arctic Canada. Palaeogeogr. Palaeoclimatol. Palaeoecol. 25, 199–207. http://dx.doi.org/10.1016/0031-0182(78)90036-6.

Williams, L.D., 1979. An energy balance model of potential glacerization of Northern Canada. Arct. Alp. Res. 11 (4), 443–456.

Wu, P., Peltier, W.R., 1984. Pleistocene deglaciation and the Earth's rotation: a new analysis. Geophys. J. R. Astron. Soc. 76, 753–791. http://dx.doi.org/10.1111/j.1365-246X.1984.tb01920.x.

Zachos, J., Pagani, M., Sloan, L., Thomas, E., Billups, K., 2001. Trends, rhythms, and aberrations in global climate 65 Ma to present. Science 292, 686–693. http://dx.doi.org/10.1126/science.1059412.

Zhang, Y.G., Pagani, M., Liu, Z., Bohaty, S.M., DeConto, R., 2013. A 40-million-year history of atmospheric CO_2. Phil. Trans. Roy. Soc. A. 371, 20130146.